Journal of Volcanology and Geothermal Research 176 (2008) 529–540

Contents lists available at ScienceDirect

Journal of Volcanology and Geothermal Research

journal homepage: www.elsevier.com/locate/jvolgeores

Geophysical investigations of the plumbing system of Stromboli volcano (Aeolian Islands, Italy)

Mario Mattia [a], Marco Aloisi [a,*], Giuseppe Di Grazia [a], Salvatore Gambino [a], Mimmo Palano [a], Valentina Bruno [a,b]

[a] Istituto Nazionale di Geofisica e Vulcanologia, sezione di Catania, Piazza Roma 2, Catania, Italy
[b] Università degli Studi di Catania, Istituto di Geologia e Geofisica, Corso Italia 55, Catania, Italy

ARTICLE INFO

Article history:
Received 20 March 2007
Accepted 29 April 2008
Available online 15 May 2008

Keywords:
Stromboli
ground deformation
modeling
plumbing system

ABSTRACT

In this work, we report the results of an integrated approach using both seismological and geodetic data provided by the INGV-CT (Istituto Nazionale di Geofisica e Vulcanologia, Sezione di Catania) Stromboli volcano monitoring systems, in order to improve the knowledge of its plumbing system. In particular, we investigated the relationships between the June 1999 seismic swarm, occurring in the area of Stromboli, and the possible activation of the NE–SW oriented volcano-tectonic structure. We analyzed this seismic swarm proposing new locations and a morphological analysis of the waveforms. This approach allowed us to demonstrate that there are relationships between the tectonic activity near Stromboli and the rising of magma. This evidence supports the hypothesis that during the 1999 swarm an intrusive process started from a crustal level where earthquakes were located (about 10–15 km b.s.l.).
As already testified by other similar episodes (deformation anomaly recorded between December 1994 and March 1995 after the November 1994 swarm), months after the 1999 seismic activity, the tiltmeters and the GPS permanent stations deployed in Stromboli, showed slow variations over three months (May–July 2000). We performed an analytical inversion of these geodetic observations and found that the modelled sources are characterized by NE–SW trend, compatible with the regional faults cutting the volcano. The modelled sources could represent the rising pathway connecting the "deep" plumbing system (about 10–15 km b.s.l.) to the "shallow" one located in the body of the Stromboli volcano (about 500 m a.s.l.).
These new evidences support the hypothesis of the existence of a simple plumbing system with different levels of magma storage, where batches of magma are periodically pushed up along the main NE–SW tectonic trend.

© 2008 Elsevier B.V. All rights reserved.

1. Introduction

Volcanic hazard at Stromboli has been analyzed in Barberi et al. (1993). It is mainly related to the effusive activity, paroxysmal explosions, but also to tsunamigenic landslides and acid rain. Recent papers have shown geophysical evidence of the existence of a shallow-level magma storage area located close to the summit area (about 500 m a.s.l.; Chouet et al., 2003; Mattia et al., 2004). The authors suggested that the almost continuous strombolian activity has its direct feeder in this area. It is worth mentioning that there are very few papers describing the geophysical aspects of the deep structures (1–10 km b.s.l.) and their relationships with the shallow magma pocket (e.g. Francalanci et al., 2004). Moreover, in the area of Stromboli very few tectonic earthquakes occur (56 earthquakes from 1885 to 1976, among which only one reached intensity VIII–IX on May 22, 1941; Falsaperla and Spampinato, 1999) and the only clear seismic signals are related to the shallow volcanic activity (tremor, low-frequency events). For this reason, any comparative study between different datasets collected during the few Stromboli tectonic seismic crises can be considered a valuable mean for constraining the plumbing system of this volcano.

In this paper, we investigate the still poorly known mechanisms of the Stromboli volcano feeding system through an integrated interpretation of continuous ground deformation signals (tilt and GPS) and seismicity. In our opinion, this methodology can lead to a holistic interpretation of the magma transfer process from depth. Thanks to the geophysical dataset collected by the INGV-CT monitoring networks (seismometers, GPS stations and tiltmeters) during and after the seismic swarm of June 1999, here we attempt to validate the models, already proposed by petrological data, of different levels of magma storage (Francalanci et al, 1989, 1993, 2004; Allard et al., 1994) or, as an alternative, of an elongated, chemically zoned and heterogeneous, dike-like feeding system (Bertagnini et al., 2003). In particular, we propose a joint analysis 1) studying in detail the 1999 seismic swarm (new hypocentral location and morphological

* Corresponding author.
E-mail address: aloisi@ct.ingv.it (M. Aloisi).

0377-0273/$ – see front matter © 2008 Elsevier B.V. All rights reserved.
doi:10.1016/j.jvolgeores.2008.04.022

waveform analysis), 2) calculating the 1999 strain tensor components from GPS data and 3) inverting the 2000 ground deformation pattern (tilt and GPS signals) in order to image the sources of these patterns.

2. Geological and volcanological setting

Aeolian magmatism must be considered in the frame of the complex geological setting at the southeastern edge of the Tyrrhenian bathyal plain. The Aeolian archipelago represents a volcanic arc of roughly one million years old related to a NE–SW striking Benioff plane (see, among others, Barberi et al., 1973; Scandone, 1979; Finetti and Del Ben, 1986; Neri et al., 2002). Since last 0.5 Ma, a wide range of volcanic products have been found, from basic to intermediate compositions, on the seven islands of the Aeolian arc. The most diffuse composition is calc-alkaline and shoshonitic (De Rosa et al., 2003; Gillot, 1987; Gillot and Villari, 1980). It is not possible to define a clear time evolution from calc-alkaline to shoshonitic magmatism, but rather a spatial distribution of magmatic affinity at the Aeolian arc scale can be observed. In particular, we observe an increase of the shoshonitic composition towards East and South, where the underlying crust is thicker and older (Gillot, 1987). Geophysical (Spakman, 1990) and geochemical (Francalanci et al., 1993) evidences suggest that magma generation is mainly derived from partial melting in the upper mantle triggered by fluid release from a subducted slab with a complex crustal contamination process.

The Stromboli Island (Fig. 1), a stratovolcano located on the northeastern end of the subaerial Aeolian arc, lies on the continental crust, which is about 20 km thick at this location (Morelli et al., 1975). To the North of the island, the Tyrrhenian basin is about 3000 m deep. The geology of the island is described in Keller et al. (1993) and Hornig-Kjarsgaard et al. (1993), and its structure is detailed in Pasquarè et al. (1993). The volcano is located along a regional NE–SW structural trend observed on fault orientations (Fig. 1) and seismic reflection profiles (Gabbianelli et al., 1993; Zanchi and Francalanci, 1989). This fault system represents the eastern branch of the Aeolian–Tindari–Letojanni fault (Ghisetti, 1979). The structural line shows normal movements and moves in response to a NW–SE striking minimum stress axis σ_3 (Tibaldi, 2001). This dominant structural feature is also testified by the lengthening of the island (Fig. 1), that is also more evident if the submerged base of the island is considered

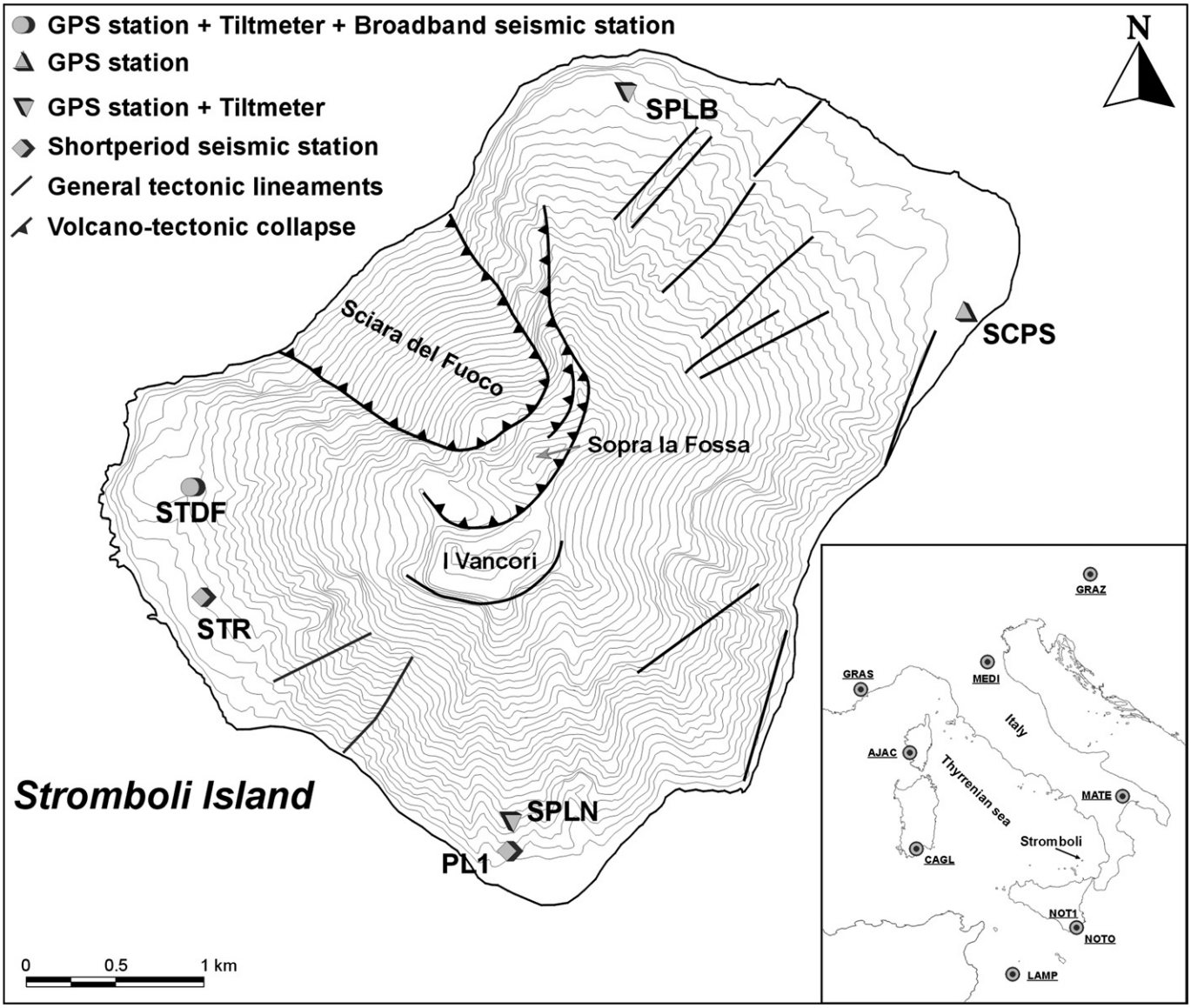

Fig. 1. Map of Stromboli volcano with the INGV-CT permanent monitoring network before 2000. In the inset are reported the 9 IGS stations included in the continuous GPS data processing. General tectonic lineaments and volcano-tectonic collapse are also reported.

(Gabbianelli et al., 1993). Minor N–S, E–W and NW–SE faults are also present (Falsaperla and Spampinato, 1999). These second-order fault systems are related to local deformations induced by sector collapses that effected the north-western sector of the edifice in the past 13 kyr (Tibaldi, 2001). The tectonic seismicity, in this sector of the Aeolian archipelago, is rather low for number and magnitude (M_{max}=3.7; Falsaperla and Spampinato, 1999).

3. The INGV-CT monitoring network

The first seismic station for monitoring purposes in Stromboli was installed in 1985 (STR, Fig. 1) and equipped with a three component, short period seismometer (1 Hz). About ten years later, a short period analogue station was added (PL1, Fig. 1). From the mid until the end of the 1990s, broadband data were available from two digital stations (STDF and PL1).

Ground deformations have been continuously monitored in Stromboli since 1992, when three tilt stations were installed in Punta Lena, Punta Labronzo and Timpone del Fuoco (SPLN, SPLB, STDF in Fig. 1; Bonaccorso, 1998). The sensors are bi-axial shallow borehole with 0.1 μrad of precision, installed at 3.5 m of depth. The two axes are respectively oriented towards the crater area (radial component) and at 90° counter-anticlockwise (tangential component).

The GPS permanent network was installed in June 1997. The remote stations (SPLN, SPLB, STDF; Fig. 1) were located at the same sites of the tilt network. In 1998, a fourth GPS station (SCPS — Scari) was added to the network, and in this way the final geometry of a polygon along the coastline, all around the cone of the volcano, was achieved. GPS data from this network are processed on a daily basis by GAMIT/GLOBK software packages (Herring et al., 2006a,b). In order to improve the overall configuration of the network and to combine the individual solutions in GLOBK, data coming from 9 IGS stations (AJAC, CAGL, GRAS, GRAZ, LAMP, MATE, MEDI, NOT1 and NOTO; Fig. 1) were also included in the processing. In the first step, double-difference and ionosphere-free linear combination of the carrier waves of the GPS signal (L1 and L2) phase observations were used to generate weighted least-square solutions for each analyzed day. The basic products of this step are GAMIT "h-files", loosely-constrained solutions containing a set of one-day site estimate positions, Earth orientation parameters and associated error covariance matrices. In the second step, the individual "h-files" GAMIT solutions are combined, by using the GLOBK Kalman filter (Herring et al., 2006b) with a regional (EURA) solution provided by the SOPAC (Scripps Orbit and Permanent Array Centre), to create a daily unconstrained combined network solution. Reference frame constraints were then applied to each daily solution by means of a Helmert transformation using the GLORG module of GLOBK. So, for each day, 7 free parameters (3 translations, 3 rotations and a scale) were estimated to minimize the derivations (by weighted least squares) between the unconstrained solution coordinates and a set of fiducial station coordinates. The basis of the global reference frame is the ITRF-2000 solution (Altamini et al. 2002). The final products are the three component time series of daily station positions with respect to ITRF-2000 reference system as well as the time series of the baselines length between the GPS stations.

4. The June 1999 swarm: seismic data

Stromboli is characterized by a variety of seismic signals (Langer and Falsaperla, 2003): 1. explosion quakes (200 per day on average); 2. major explosions (2 per year on average); 3. volcanic tremor and 4. rare tectonic earthquakes. We focused on this last category because we are interested in demonstrating that there are relationships between the tectonic activity near Stromboli and the rising of magma. In the last twenty years, only three swarms have been recorded by the INGV-CT seismic network: in November 1994 (8 events, max Md=3.7), between 6 and 17 June 1999 (78 events, max Md=3.2) and in April–May 2006 (6 events, max Md=3.3). In particular, we analyze the swarm of June 1999 because it is the biggest (both in number of events and for the released energy) and because some of its characteristics can be related to a magmatic intrusion from depth. Fig. 2 illustrates that the strain released in the Stromboli area is low (in accordance with the low number of tectonic or volcano-tectonic seismic events). We hypothesise that the hypocentral locations (6 km NE of the volcano, between 8.5 and 11.2 km of depth) proposed by Falsaperla et al. (2003) for the main shocks of the June 1999 swarm are not reliable (see stars in Fig. 3). We think that the focal volume of the swarm is not NE of the island but rather localized in the body of the volcano. In the Stromboli area, a good estimation of the hypocenters based on standard least-square techniques applied to arrival times (e.g. Hypo71 or Hypoellipse

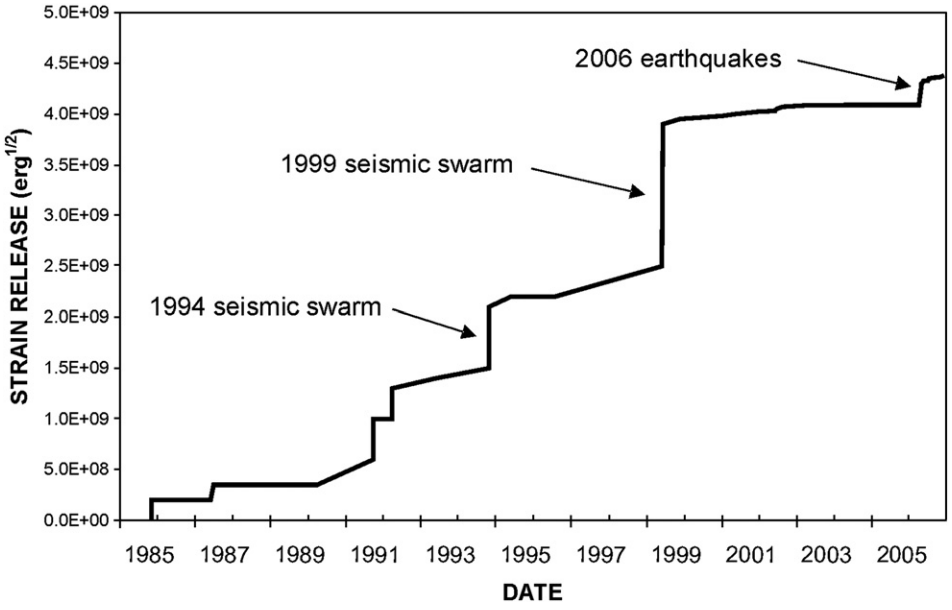

Fig. 2. Cumulative strain release in Stromboli area from June 1985 to December 2006 (modified from Falsaperla et al., 2003).

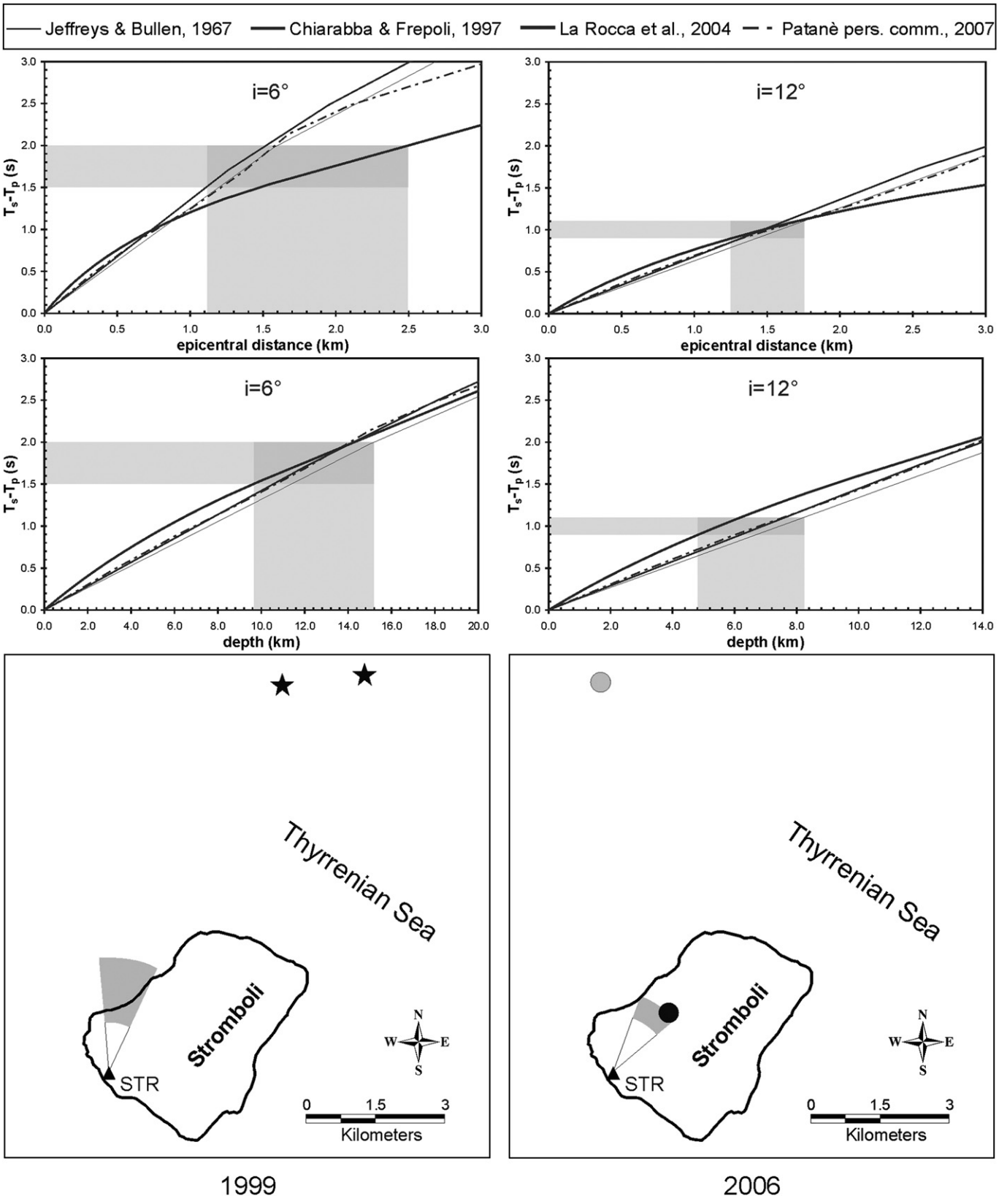

Fig. 3. Hypocentral location obtained by ray-tracing method. On the left: theoretical *Ts–Tp vs. epicentral distance* (top) and *Ts–Tp vs. depth* (middle) plots on the basis of four different velocity models. Grey colours mark epicentral distance and depth ranges achieved by the observed Ts–Tp data for an average angle of incidence of 6° or 12°. At the bottom-left: the resulting epicentral area (grey) for the 1999 seismic swarm, compared to the best analytical epicentres (stars) reported in Falsaperla et al., 2003. At the top and middle right: the same as on the left for the 2006 earthquakes. An average angle of incidence of 12° was assumed. The 2006 epicentral area (grey at bottom-right) is compared to best location (at about 6 km of depth) based on travel-time residuals method (black circle). Grey circle indicates the localization of the same earthquake achieved with a seismic network set as in 1999. Data from Jeffreys and Bullen (1967), Chiarabba and Frepoli (1997), La Rocca et al. (2004) and Patane (pers. comm., 2007).

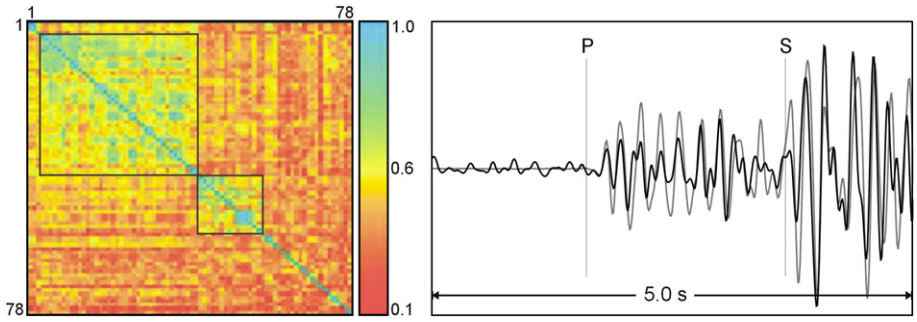

Fig. 4. On the left: correlation matrix for the 78 analyzed earthquakes at STR station. A colour scale bar, related to correlation coefficient values, is shown. The squares mark the two detected families (see text). On the right: as an example, two earthquakes of duration magnitude of 3.2 (grey) and 2.4 (black) with cross-correlation value of 0.77 are reported. Amplitudes of seismic signals are normalized.

software; Lahr, 1989) is very difficult mainly for two reasons: 1. the geometry of the network is limited to the emerged part of Stromboli; 2. the still poorly known velocity models in this area. Here, we performed a single-station hypocentral localization by mean of a ray-tracing technique, using the signals from STR station (Fig. 1). Considering the hypothesis of an isotropic medium, the method consists in tracing back, from receiver to source, the ray path, knowing its back-azimuth, angle of incidence, P and S arrival times and assuming a velocity model. We make use of Snell's law (Alessandrini et al., 1994). As Ts–Tp time differences were clearly readable from seismograms, back-azimuth and apparent angles of incidence at receiver were achieved by polarization analysis of the unfiltered three component seismic signals, using the CMD (Covariance Matrix Decomposition) algorithm (Montalbetti and Kanasewich, 1970; Patané and Ferrari, 1997). True angles of incidence were obtained from the apparent ones by applying relations provided by the elasticity theory for a plane P-wave reflected on a horizontal free surface (Alessandrini et al., 1994). No interaction of seismic waves with topography was taken into account.

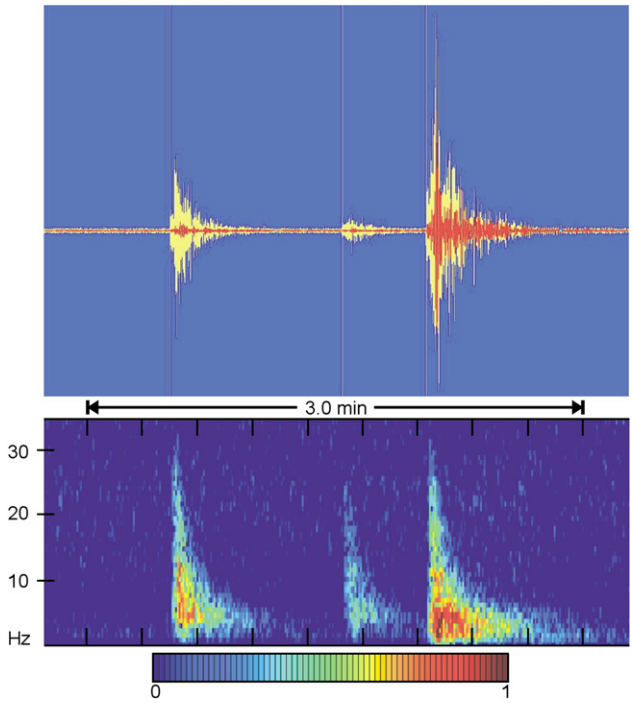

Fig. 5. Top: sequence of three earthquakes (yellow) occurring on June 13, 1999. In red, the same sequence after applying a 2.5 Hz low pass filter. The different amplitude attenuation of seismograms evidences that the third seismic event is characterized by lower frequencies than the other ones. Bottom: spectrogram obtained by 128-points FFT with 50% overlap. The different frequency content of the last event is enhanced. This event, characterized by high-frequency onset followed, a few seconds later, by lower frequencies than the other ones, is presumed to be a "hybrid" event. (For interpretation of the references to colour in this figure legend, the reader is referred to the web version of this article.)

Most of the strongest earthquakes of the June 1999 swarm (Md ≥ 2.5; 31 of 78) presented the following parameters: back-azimuth between N355°E and N25°E; apparent angle of incidence between 2° and 8°; Ts–Tp between 1.5 s and 2.0 s. We rejected 12 of the 31 events whose values were poorly constrained (confidence limits at 95% > 20° for azimuth and/or 5° for incidence; for details see Patané and Ferrari, 1997). The hypocentral locations obtained by ray-tracing methods proved more dependent on the velocity model used than those calculated using the standard least-square techniques applied to arrival times. Then, starting from an average angle of incidence, we calculated Ts–Tp theoretical curves with respect to both epicentral distance and depth for four different velocity models (Fig. 3). In this way, based on the observed Ts–Tp, together with back-azimuth, we were able to establish an alternative location of 1999 seismic swarm (grey area on the bottom-left, Fig. 3; depth between 10 and 15 km b.s.l.).

With the aim of testing the reliability of this location, we applied the same procedure to the 2006 earthquakes, well located, using standard least-square techniques, between 4 and 6 km of depth below the island (INGV, Sezione di Catania Reports; www.ct.ingv.it; D'Auria et al., 2006). We are able to use the standard techniques, thanks to the presence of a permanent network of 12 broadband digital seismic stations deployed since January 2003. Results are shown in Fig. 3 (grey area on the bottom-right) and compared to analytical hypocentral locations (black circle) attained by means of Hypoellipse software. The two different methods provide very similar hypocentral locations. Conversely, a very different analytical hypocentral location is obtained if we use a seismic network configuration as in 1999 (grey circle; Fig. 3). It is worth remarking that hypocentral solutions for the most vigorous events of 2006 are very close to those of Falsaperla et al. (2003) (most vigorous events of 1999 swarm), using a 1999 similar seismic stations configuration (see stars and grey circle in Fig. 3). This test confirms that in the 1999 case, the seismic network geometry is inadequate to obtain a reliable location, using standard least-square techniques applied to arrival times.

Moreover, with the aim of studying the relationships between the Stromboli tectonic activity and the magmatic fluids, we performed a morphological analysis of the 1999 swarm waveforms. Clustered events often produce similar seismograms, as a result of a common source mechanism as well as common path and site effects. Tsujiura (1983) suggested that such families of events, called multiplets, are characteristic of earthquake swarms due to repeated slip on the same fault plane. These events have been associated with both tectonic (Poupinet et al., 1984) and volcanic activities (Got et al., 1994). Many of the 78 seismic events of the June 1999 swarm show a good morphological similarity of the waveforms, as already reported in Falsaperla et al. (2003). We tried to improve this morphological analysis thanks to a statistical approach named "bridging technique" (Cattaneo et al., 1999) aimed at clustering

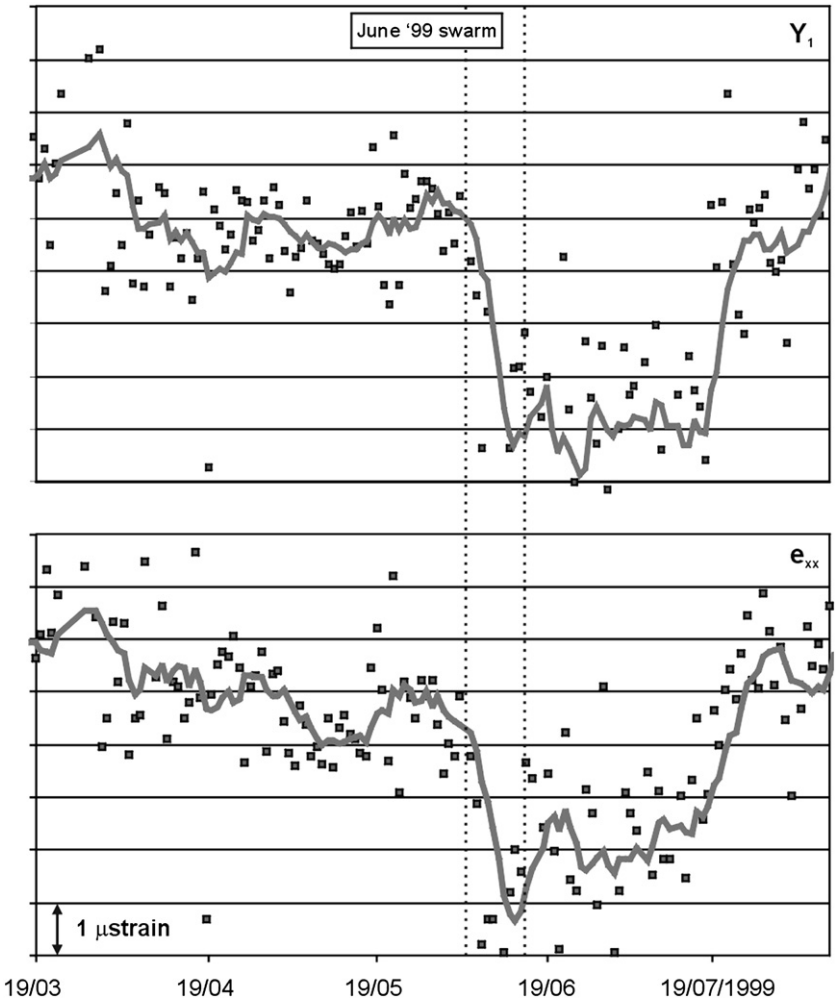

Fig. 6. Y_1 and e_{xx} strain tensor components (the squares represent daily values and the grey line is an interpolation curve). Dashed vertical lines indicate the 1999 June swarm period.

events into families. If two couples of events (x, y) and (y, z), exceeding the correlation threshold, share a common quake (y), the method considers that all three events pertain to the same family, even if the correlation (x, z) is below the threshold. In order to easily evaluate the similarity of waveforms, we chose to apply the cross-correlation analysis over 2.5 s of each seismogram. This time window allowed the inclusion of both P and S phases for the whole dataset. On the basis of a correlation threshold fixed at 0.7, we found two different families, as shown in the cross-correlation matrix, composed of 38 and 16 volcano-tectonic events, respectively (Fig. 4). The remaining 24 events did not show meaningful correlation with both families and most of them were characterized by relatively low-frequency content and they are called "hybrids". As an example, Fig. 5 shows a sequence of three events occurring in a couple of minutes duration with magnitude 2.6, 2.2 and 3.0, respectively. The different frequency content is evidenced by both the FFT analysis and the different amplitude attenuation of the three filtered signals, applying a 2.5 Hz low pass filter. The third event is clearly characterized by lower frequencies and is a hybrid earthquake. Hybrid events have been found at many volcanoes and have an intermediate waveform feature between high-frequency volcano-tectonic

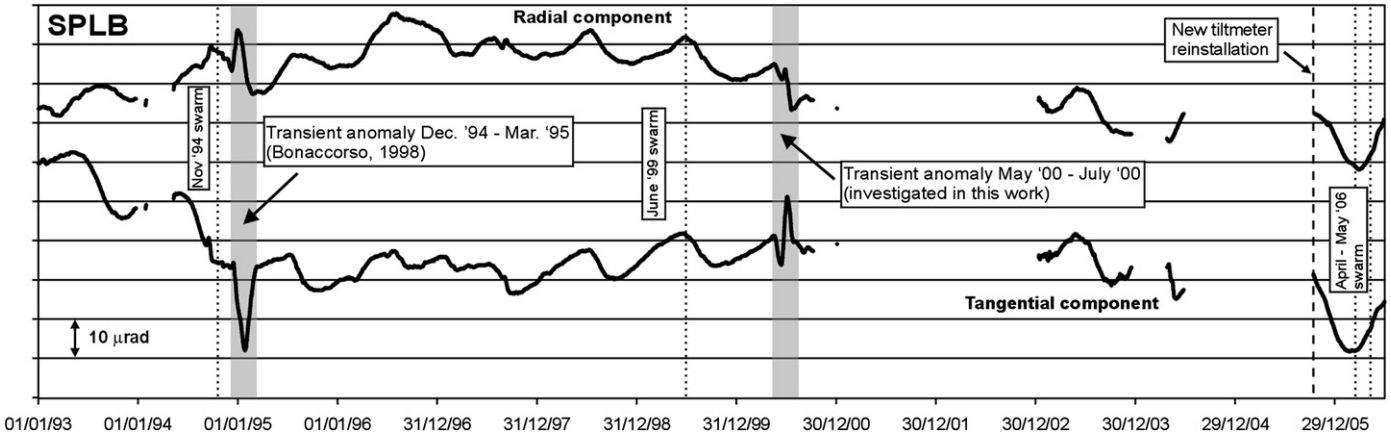

Fig. 7. SPLB tilt signal recorded from 1993 to 2006.

Table 1
Estimated parameter and uncertainties

Parameter	Phase I	Phase II	Phase III	Phase IV
Lat (m)	518,509±358	517,789±178	517,521±302	518,592±341
Long (m)	4,296,669±368	4,296,095±123	4,295,792±202	4,296,514±365
Azimuth (deg)	−134.6±4.4	−139.4±4.6	−134.0±4.9	−135.6±4.7
Ztop (m)	−1638±372	−1126±279	−915±307	−1846±343
Length (m)	1562±337	1418±217	1534±332	1764±340
Width (m)	629±329	1516±341	765±331	463±278
Dip (deg)	40.3±5.0	48.9±4.7	40.3±4.8	39.7±4.8
Strike-slip (m)	−0.02±0.10	−0.12±0.11	−0.21±0.11	−0.01±0.10
Dip-slip (m)	0.10±0.10	0.12±0.11	0.11±0.11	0.10±0.10
Opening (m)	0.85±0.11	0.96±0.10	0.85±0.11	0.85±0.11

Coordinates in UTM (WGS84). The reference surface ($z=0$) has been assumed at the sea level, which is approximately the altitude of stations used in the inversion.

earthquakes and long period (LP) events. Generally, the higher frequency energy preceded the LP phase by about 3–4 s and presented an impulsive onset and linear polarisation, typical of P-waves. This allowed the use of standard travel-time difference methods and/or particle motion analysis to locate these events. As their hypocentral location was not significantly different from the other events of the swarm, we supposed that their low-frequency nature is attributable to source rather than to path or site effect. For hybrid events, Lahr et al. (1994) hypothesized the contemporaneous fracturing of rocks and excitation of fluids (double couple and volumetric mechanisms), due to the presence, in the focal volume, of magmatic and/or hydrothermal fluids. Although such events frequently occur at the initial stage of activation of a volcano, especially during explosive activity, their origin is controversial. The hybrid earthquakes represent a superposition of two events of differing nature (Gordeev and Senyukov, 2003): 1. a common volcano-tectonic earthquake originated by crack propagation driven by overpressure-induced stress overcoming critical levels, and 2. low-frequency volumetric vibration of gas-saturated magma, excited by an elastic reaction of the surrounding media due to crack growth and/or oscillation of a fluid-filled crack (Chouet, 1996). In any case, such processes imply the presence of a magma body in contact with the fracturing surrounding rocks, as most likely happened at Stromboli during the 1999 seismic swarm.

5. The June 1999 swarm: geodetic data

A further proof of the proposed interaction between seismic activity and magmatic fluids, with the aim to define the path for magma rising, could be provided by the temporal analysis of the strain tensor components calculated using the 1999 length variations recorded at the baselines of the continuous Stromboli GPS network. The strain tensor, calculated assuming that the strain field is uniform, is an efficient representation of the deformation pattern. It represents an average value of the strain at work with the aim of providing an overall pattern of the deformation effects (Livieratos, 1980). In the plane infinitesimal strain theory, the deformation is described by the following bidimensional Jacobian characterizing the transformation linking the coordinate space (x, y) to the corresponding space of the displacement (u, v), (Livieratos, 1980):

$$e_{ij} = e_{ji} = \begin{bmatrix} e_{xx} & \frac{1}{2}Y_2 \\ \frac{1}{2}Y_2 & e_{yy} \end{bmatrix}$$

The strain tensor components have the following physical meaning: e_{xx} is the change of length per unit of length in the East direction, positive for extension; e_{yy} is the change of length per unit of length in the North direction, positive for extension. Moreover, Y_1 defined as $(e_{xx}-e_{yy})$ is the shear across any line parallel to the NW–SE line, positive for right lateral shear. Y_2 defined as $(e_{xy}+e_{yx})$ is the shear across any line parallel to the East axis, positive for right lateral shear where e_{xy} is the shear across any line parallel to the E direction, positive for right lateral shear. From the composition of these parameters, we can define the quantity $\Delta=e_{xx}+e_{yy}$, called areal dilatation. It represents the change of area per unit of area, positive for increase in area.

During the seismic swarm between 6 and 17 June 1999, the e_{xx} component, analogously to the shear component Y_1, shows a negative trend (Fig. 6). No evident variations are shown by the Y_2 shear component trend. The areal dilatation, highly influenced by the e_{xx} pattern, shows a mean negative variation also (areal compression) in that period (about 2 μstrain). In our opinion, despite the small variation entities, the strain tensor components could be related to the 1999 tectonic earthquakes. It's difficult to compare the values of strain induced by the swarm and the observed geodetic strain mainly for two reasons: 1. the geodetic strain span a period of several days where the movements can be assumed as slow and continuous 2. we haven't enough data and information about, for example, the focal volume of the swarm, that are indispensable for a correct estimation of the released seismic strain. From the observed geodetic variations of strain parameters we can assume that these movements are compatible with a left striking movement on a NW–SE fault or a dextral striking movement on a NE–SW fault. Referring to the structural lineaments prevailing in Stromboli area (e.g. Gabbianelli et al., 1993; Zanchi and Francalanci, 1989;), the most probable direction of movement is NE–SW and the shear components should be dextral. Then, the probable path for magma rising seem to be the regional NE–SW trending faults system.

6. Inversion of geodetic data

The June 1999 seismic swarm re-analysis, allowed us to reveal that there are relationships between tectonic activity and magmatic fluids in Stromboli area at a depth between 10 and 15 km (crustal levels), along the regional NE–SW structural trend.

About a year after the 1999 seismic activity, the tiltmeters and the GPS permanent stations, deployed in Stromboli, showed slow variations during three months (from May to July 2000; Fig. 7). A similar behaviour (earthquakes swarm and, after months, magmatic intrusion) was recorded after the 1994 swarm also (Bonaccorso, 1998). Here, we modelled the 2000 geodetic transient anomaly with the aim of verifying if it is interpretable as a magma migration from crustal levels, starting during the 1999 seismic swarm, toward shallow-level magma storage area located close to the summit area (about 500 m a.s.l.; Chouet et al, 2003; Mattia et al., 2004).

We used the dislocation theory in a semi-infinite, homogeneous, isotropic and elastic body to calculate displacements and tilt at each station, caused from a tabular dislocation model (Okada, 1985). We estimated 10 parameters for each dislocation structure: coordinates of the top (Lat, Long, Ztop), dimensions (length and width), orientation (azimuth and dip) and displacements (strike-slip, dip-slip, opening). The inversion is performed using a least squares method (Tarantola and Vallette, 1982). In order to verify the stability of our solution and to solve minimum problems, we also repeated the analytical process for thousands of models in the space of the parameters with a grid-search technique, testing these results by the χ^2 test.

We inverted all the available data recorded by the continuous GPS and tilt network (Fig. 1) from May to July 2000. In particular, during this period, tilt changes of tens of μrad were detected on Stromboli's northeastern flank. SPLB tilt signals recorded some reversals in both the radial and tangential components (Fig. 7). These data allowed us to constrain the position of the deformation source at that time. In fact, from theory (Bonaccorso and Davis, 1993), a reversal in tilt can occur when a dike passes the point where a tilt station projects onto the plane of the dike. Stromboli borehole tiltmeters have a nominal precision in the order of 0.1 μrad. The real precision, however, may be

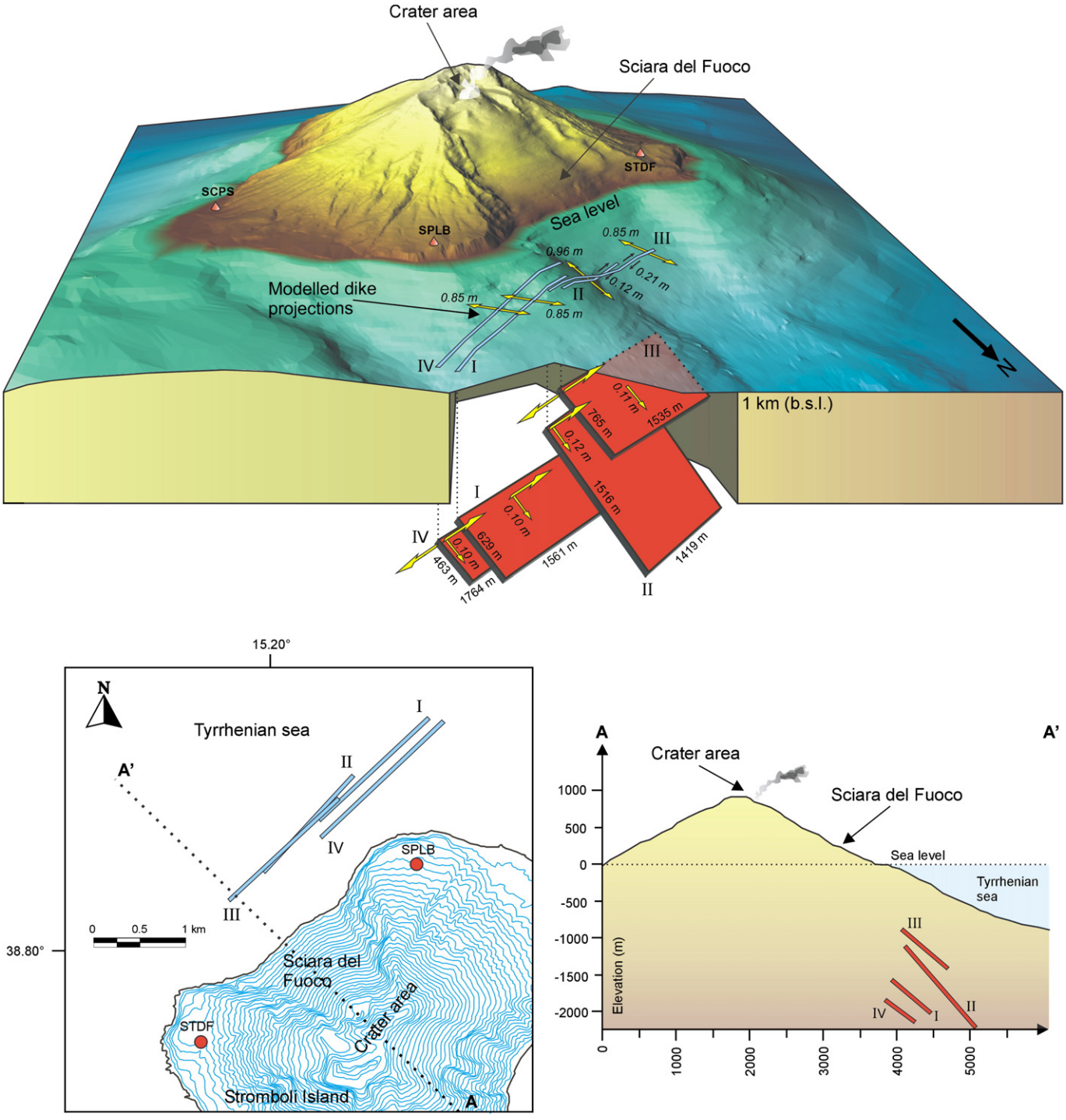

Fig. 8. Three-dimensional model sketch of the intrusion producing the Stromboli 2000 geodetic anomaly. Projection of the estimated four phases in plane and cross-sectional views are also reported.

affected by noise due to poor siting, meteorological fluctuations and long-term instrument drift. These effects are more marked in the SPLN tiltmeter signals; then, real precision at this station is ca. 2 μrad. No variation greater than noise was observed at SPLN during the investigated period. We used this information as a model constraint during the inversion of the geodetic data. Regarding STDF tiltmeter, severe electronic noise affected tilt signals during 2000; for this reason these data are unusable. Small variations (a few centimetres) were recorded at the GPS permanent network. The deformation pattern was characterized by a very small contraction. In particular, SPLB, SCPS and SPLN GPS stations showed a centimetric displacement toward SE while smaller variations were recorded at STDF station. A general centimetric downlift was also recorded. Altogether, we inverted the displacement components recorded by four GPS stations and the tilt components revealed by two borehole clinometers.

The reversals observed on the SPLB tilt signals allowed identifying four different phases during the Stromboli 2000 geodetic anomaly: the first (I) from 17 May '00 to 14 June; the second (II) from 14 June to 27 June; the third (III) from 27 June to 4 July; the fourth (IV) from 4 July to 25 July. Separate analyses were performed for each phase. In order to obtain a starting model for the first phase, we performed a search in the space of the parameters with a grid-search technique, testing these results by

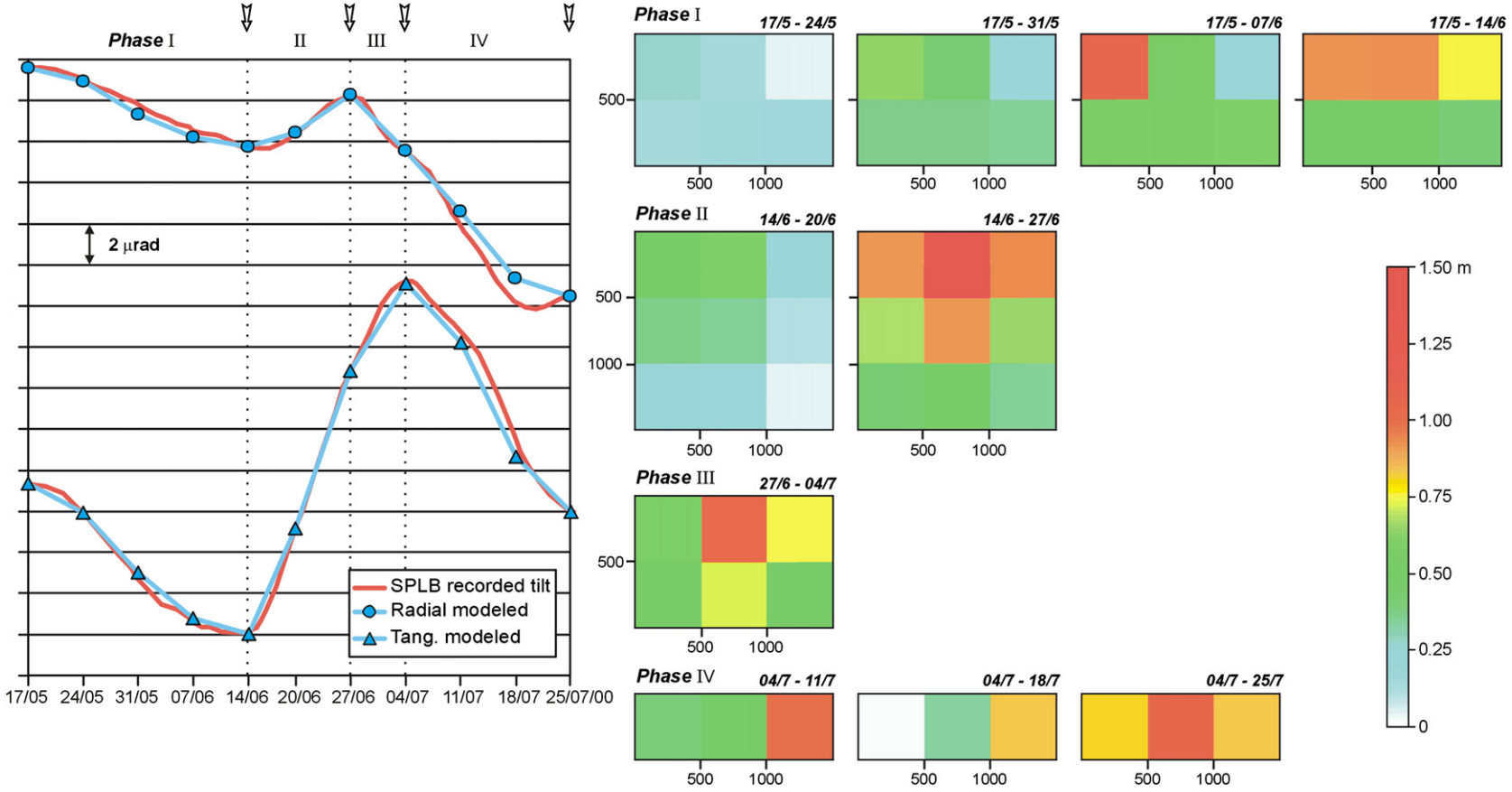

Fig. 9. Spatial and temporal distribution of dike opening component for each phase. Modelled and recorded signals at the SPLB tilt station are also reported.

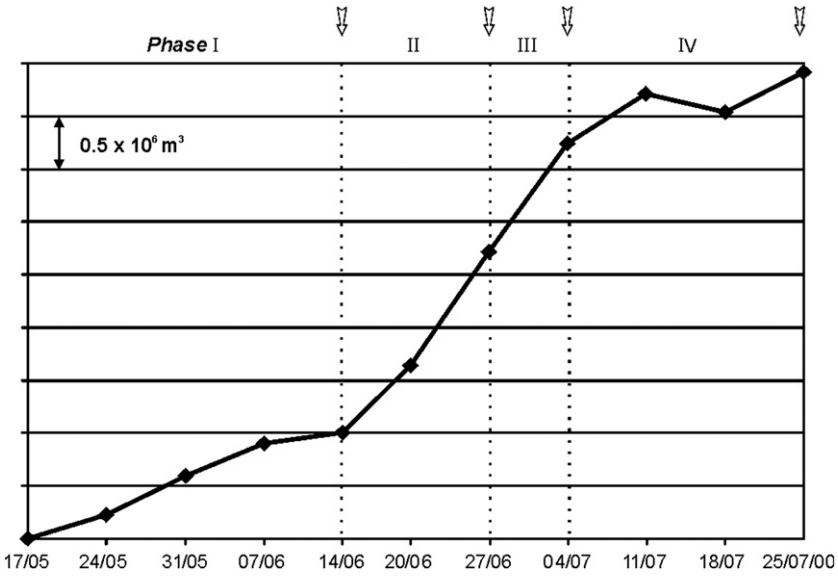

Fig. 10. Modelled temporal change of the volume of the intrusion for all phases.

the χ^2 test. Then, we used the least squares method (Tarantola and Vallette, 1982) to image the deformation pattern recorded from 17 May '00 to 14 June. The obtained final model was used as the starting model for the next least squares inversion related to the second phase and so on for the following two phases. Table 1 reports the estimated model parameters for each phase. The source parameter uncertainties have been calculated as the standard deviation in the class of all the solutions that satisfy the χ^2 test for our degrees of freedom within the significance level of 5%. The modelled sources, reported in Fig. 8, are characterized by the same NE–SW trend and a NW-dipping low dip angles (ranging from about 40° to 50°), compatibly with the regional NE–SW trending system faults, cutting the volcano. Furthermore, all the sources are dominated by an opening component ranging between 0.85 and 0.96 m, coupled with minor dip-slip and strike-slip components (see Table 1 for details). The overall recorded deformation pattern seems compatible with a deformation source migration from NE to SW (Fig. 8) and also with a progressive uprising (from phases I to III; Fig. 8 and Table 1). It is noteworthy, that for the fourth stage we obtained a very similar dislocation to the first one. We believe that this phase represents a successive refilling of the deeper system.

We believe that, during the 1999 seismic hybrid swarm, an intrusive process started at crustal levels, as testified by the earthquakes depth (between 10 and 15 km b.s.l.). In this framework, the modelled 2000 geodetic transient anomaly could be due to the uprising of the same magmatic fluids involved in the 1999 swarm, from crustal levels toward the emerged body of the volcano, along the main NE–SW tectonic trend.

Moreover, to better define the magma migration process, we propose a temporal analysis of the opening component (Irwan et al., 2006). Dividing the obtained tabular dislocations into a grid of uniformly sized blocks of 500×500 m, we inverted for the opening component solely, using a least squares criterion (Tarantola and Valette, 1982) with a weekly frequency. We used all geodetic data available (displacement components for the four GPS stations and tilt components for the two clinometers). The results are shown in Fig. 9 together with the modelled and recorded signals at the SPLB tilt station. The highest intrusion opening value was about 1.5 m and was reached during the second phase. We can observe that the opening component is smaller in the deeper zone of the intrusion planes (dikes) with respect to the shallower one. The tensile component, mainly evident in the upper parts of the dikes, could confirm a process of forceful intrusion in a weak structural alignment (the NE–SW trending system faults). We also calculated the weekly intrusion volume change for all phases (Fig. 10). The total amount of intruded magma is about $4.5*10^6$ m^3, a small quantity, comparable with the estimated lava output during the 1985 eruption ($5–6*10^6$ m^3 from De Fino et al., 1988), but greatly inferior to the total estimated amount of emitted lava for the 2002–2003 eruption ($11*10^6$ m from Landi et al., 2006).

The intrusion of May–July 2000 was slow, lasted about three months and did not lead to an eruption. During the overall ascent from depth toward shallower levels, small dimensions of magma batches were supplied. We can observe that the time intrusion showed different evolution velocity (Fig. 10). The initial and last phases were characterized by a similar velocity of intrusion (Fig. 10). Moreover, the last phase showed an "intermittent" behaviour, most likely caused by the slow level of associated energy. The central phases were faster and involved the greatest volume of magma.

7. Discussion and conclusions

In this study we summarized the main geophysical data collected during and after the June 1999 seismic swarm, with the aim of 1. demonstrating that the regional NE–SW striking fault crossing the Stromboli volcano is periodically injected from depth with new batches of magma that rise up along the same discontinuity, until the shallow magma pocket located above sea level; 2. imaging the structures affected by this process of magma transfer; 3. improving the knowledge on the limits and perspectives of the monitoring system currently running on Stromboli.

During the June 1999 swarm, we recognized the clear presence of events, called "hybrids" (Fig. 5). Such processes imply the presence of magma bodies in contact with the fracturing surrounding rocks. The contemporaneous changes observed in the strain tensor parameters (Fig. 6) are compatible with a dextral shear movement along a NE–SW direction. This aspect suggests the interesting possibility of the activation of the volcano-tectonic structure oriented NE–SW, representing the structural lineaments prevailing in Stromboli area, together with magmatic fluid movements.

About a year after the 1999 seismic swarm, the continuous geodetic network recorded a transient anomaly, over three months (May–July 2000; Fig. 7). A similar anomaly was recorded from December 1994 to March 1995, after the 7 November 1994 seismic swarm (see Bonaccorso, 1998). The author hypothesized a dike intrusion related to the 1994 seismic swarm, modelling the tilt signal

with a NE–SW directed progressive intrusion at a depth of about 1200 m.

In this work, we modelled the temporal evolution of the ground deformation pattern, recorded by the Stromboli permanent geodetic network from May to July 2000 (Fig. 7). This was done to verify if this event might be closely related to the 1999 seismic swarm, representing (as already observed in Bonaccorso, 1998) a process of forceful intrusion revealed by geodetic networks only when magma reaches shallower levels.

By looking at the results of the ground deformation inversions, the inferred dikes (Fig. 8) are characterized by a NE–SW trend that is compatible with the dominant structural feature affecting the Stromboli volcano area. This structural characteristic corresponds to the eastern branch of the Aeolian–Tindari–Letoianni fault system. In addition, the modelled dip-slip and strike-slip components (showing respectively, normal and dextral movement) are compatible with the kinematic behaviour of the eastern branch of the Aeolian–Tindari–Letoianni fault system (Ghisetti, 1979). Furthermore, these results are in good agreement with those obtained by De Astis et al., (2003) who, applying a simple mechanical model, constrained by field structural data, demonstrated that an extensional stress field with a NW–SE striking σ_3 acts in this area, allowing the opening of NE–SW striking cracks. In light of this, we retain that the volcanic activity of Stromboli is linked to the activation of the eastern branch of the Aeolian–Tindari–Letoianni fault system. We think that the dual interpretation regarding whether the eastern branch tectonic seismicity leads to the magma intrusion or conversely the magma intrusion leads to tectonic stress is unsolved with the available data.

The activation of the NE–SW faults system, as testified by the 1999 hybrid earthquakes, was observed together with a magma injection (between 10 and 15 km b.s.l.), reaching, after about one year, the depth of about 1–2 km (Fig. 8), just beneath the shallow plumbing system located in the body of the volcano (about 500 m a.s.l.; Chouet et al, 2003; Mattia et al., 2004). In this framework, the modelled sources could represent the ascent pathways connecting the deep plumbing system located between 10 and 15 km of depth (1999 new hypocentral location) to the shallow one located in the body of the Stromboli volcano (about 500 m a.s.l.; Chouet et al, 2003; Mattia et al., 2004).

Regarding the seismicity during the 2000 geodetic anomaly, unfortunately, over the period of the measured ground deformation between May and July 2000, the local seismic network was down and we cannot report any possible seismicity related to the intrusive process. The INGV national seismic network only reports one event of magnitude Md>2.5 occurring on 17 June 2000 and localized South–West of Stromboli Island.

Moreover, regarding the volume of the intruding magma, the small total amount (about $4.5*10^6$ m^3; Fig. 10) testifies to the small quantity of energy involved when little batches of magma are periodically forced up along the main NE–SW tectonic trend that cuts the volcano (Figs. 8 and 10), as shown by the fourth phase (Fig. 10) that, being very similar to the first phase, should represent a successive refilling of the deeper system. It is likely that the small quantity of intruded magma, if compared with the volume of magma erupted in the 2002–2003 eruption ($11*10^6$ m from Landi et al., 2006), can be justified assuming that the event of forceful intrusion between 1999 and 2000 is visible only because it was larger than other small magma inputs, not detected by geodetic data. Also, the very low-magnitude seismic events related to these smaller intrusions could be masked by the highly vigorous and continuous explosive activity of the volcano.

In conclusion, we believe that when the NE–SW structural line moves showing a dextral shear component as testified by the seismic "hybrid" activity and geodetic strain tensor components analysis, contemporarily magmatic fluids find a way to ascend from crustal levels (about 10–15 km b.s.l.) and refill a more shallow storage area that we have modelled here (between about 1 and 2 km b.s.l.). Successively, from this depth, the magma rises up toward the shallow-level storage area located close to the summit area (about 500 m a.s.l; Chouet et al, 2003; Mattia et al., 2004), where the almost continuous strombolian activity has its direct feeder.

The Stromboli monitoring geodetic network, located in the subaerial volcano flanks and representing only the extreme vertex of the whole edifice, is able to only show us this final part of the overall magma uprising process. This may explain the time span between the seismicity and the intrusive processes at shallower levels (above 1–2 km b.s.l.). Tilt data was very useful at Stromboli for two main reasons: 1. the small dimension of the supplied magma batches; 2. the sensitivity of GPS measurements. Indeed, the precision levels of the GPS technique and the data scattering due to the various noise sources (thermoelastic effects, sea tides, earth tides, multipath, etc.) can mask the small but significant variations of the Stromboli ground deformation pattern.

Finally, the discussion on the petrological implications of the suggested feeding system is beyond the scope of this work. However, we retain that the substantially simple proposed plumbing system is compatible with the petrological and geochemical data, thus suggesting that Stromboli's feeding system must be characterized by different levels of magma storage at different depths (Francalanci et al., 2004; Allard et al., 1994; Vaggelli et al. 2003).

Acknowledgments

The authors are grateful to the Associate Editor, Jurgen Neuberg, and to two anonymous reviewers for their constructive suggestions. This work was partially funded by the Italian Dipartimento della Protezione Civile in the frame of the 2004–2006 Agreement with Istituto Nazionale di Geofisica e Vulcanologia — INGV (Project V2 "Stromboli" task 14).

References

Alessandrini, B., Cattaneo, M., Demartin, M., Gasperini, M., Lanza, V., 1994. A simple P-wave polarization analysis: its application to earthquake location. Annali di Geofisica XXXXVII (5).

Allard, P., Carbonnelle, J., Metrich, N., Loyer, H., Zettwoog, P., 1994. Sulphur output and magma degassing budget of Stromboli volcano. Nature 368, 326–330.

Altamini, Z., Sillard, P., Boucher, C., 2002. ITRF2000: a new release of the International Terrestrial Reference Frame for earth science applications. J. Geophys. Res. 107 (B10), 2214. doi:10.1029/2001JB000561.

Barberi, F., Gasparini, P., Innocenti, F., Villari, L., 1973. Volcanism of the Southern Tyrrhenian Sea and its geodynamic implications. J. Geophys. Res. 78, 5221–5232.

Barberi, F., Rosi, M., Sodi, A., 1993. Volcanic hazard assessment at Stromboli based on review of historical data. Acta Vulcanologica 3, 173–187.

Bertagnini, A., Métrich, N., Landi, P., Rosi, M., 2003. Stromboli volcano (Aeolian Archipelago, Italy): an open window on the deep-feeding system of a steady state basaltic volcano. Journal Geophysical Research 108 (B7), 2336. doi:10.1029/2002JB002146.

Bonaccorso, A., 1998. Evidence of a dyke-sheet intrusion at Stromboli volcano inferred through continuous tilt, Geophys. Res. Lett. 25 (22), 4225–4228.

Bonaccorso, A., Davis, P.M., 1993. Dislocation modelling of the 1989 dike intrusion into the flank of Mount Etna, Sicily. J. Geophys. Res. 98, 4261–4268.

Cattaneo, M., Augliera, P., Spallarossa, D., Lanza, V., 1999. A waveform similarity approach to investigate seismicity patterns. Nat. Hazards 19, 123–138.

Chiarabba, C., Frepoli, A., 1997. Minimum 1D velocity models in Central and Southern Italy: a contribution to better constrain hypocentral determinations. Ann. Geophys. XL (4) August 1997.

Chouet, B.A., 1996. Long-period volcano seismicity; its source and use in eruption forecasting. Nature 380 (6572), 309–316 illus., 77 refs.

Chouet, B., et al., 2003. Source mechanisms of explosions at Stromboli determined from moment tensor inversion of very long period data. J. Geophys. Res. 108, 2019–2044 doi: 10.129/2002JB001919, 2003.

D'Auria, L., Giudicepietro, F., Martini, M. and Orazi, M., 2006. The April–May 2006 volcano-tectonic events at Stromboli volcano (Southern Italy) and their relation with the magmatic system. Earth-Prints open archive: http://www.earth-prints.org/handle/2122/1506.

De Astis, G., Ventura, G., Vilardo, G., 2003. Geodynamic significance of the Aeolian volcanism (Southern Tyrrhenian Sea, Italy) in light of structural, seismological, and geochemical data. Tectonics 22 (4), 1004. doi:10.1029/2003TC001506.

De Fino, M., La Volpe, L., Falsaperla, S., Frazzetta, G., Neri, G., Francalanci, L., Rosi, M., Sbrana, A., 1988. The Stromboli eruption of December 6, 1985–April 15, 1986: volcanological, petrological and seismological data. Rend. Soc. Ital. Mineral. Petrol. 43, 1021–1038.

De Rosa, R., Guillou, H., Mazzuoli, R., Ventura, G., 2003. New unspiked K–Ar ages of volcanic rocks of the central and western sector of the Aeolian Islands: reconstruction of the volcanic stages. J. Volcanol. Geotherm. Res. 120, 161–178.

Falsaperla, S., Spampinato, S., 1999. Tectonic seismicity at Stromboli volcano (Italy) from historical data and seismic records. Earth Planet. Sci. Lett. 173, 425–437.
Falsaperla, S., Alparone, S., Spampinato, S., 2003. Seismic features of the June 1999 tectonic swarm in the Stromboli volcano region, Italy. J. Volcanol. Geotherm. Res. 125, 121–136.
Finetti, I., Del Ben, A., 1986. Geophysical study of the Tyrrhenian opening, Boll. Geof. Teor. Appl. 28, 75–155.
Francalanci, L., Manetti, P., Peccerillo, A., 1989. Volcanological and magmatological evolution of Stromboli volcano (Aeolian islands): the roles of fractional crystallisation, magma mixing, crustal contamination and source heterogeneity. Bull. Volcanol. 51, 355–378.
Francalanci, L., Taylor, S.R., McCulloch, M.T., Woodhead, J.D., 1993. Geochemical and isotopic variations in the calcalkaline rocks of Aeolian arc, southern Tyrrhenian Sea, Italy: constraints on magma genesis. Contrib. Mineral. Petrol. 113, 300–313.
Francalanci, L., Tommasini, S., Conticelli, S., 2004. The volcanic activity of Stromboli in the 1906–1998 AD period: mineralogical, geochemical and isotope data relevant to the understanding of the plumbing system. J. Volcanol. Geotherm. Res. 131, 179–211.
Gabbianelli, G., Romagnoli, C., Rossi, P.L., e Calanchi, N., 1993. Marine geology of the Panarea–Stromboli area (Aeolian Archipelago, Southeastern Tyrrhenian sea). Acta Vulcanol. 3, 11–20.
Ghisetti, F., 1979. Relazione tra strutture e fasi trascorrenti e distensive lungo i sistemi Messina–Fiumefreddo, Tindari–Letojanni e Alia–Malvagna (Sicilia nord-orientale): uno studio microtettonico. Geol. Romana 11, 35–42.
Gillot, P.Y., 1987. Histoire volcanique des Iles Eoliennes: arc insulaire or complexe orogenique anulaire? D.T. IGAL 11, 35–42, 106.
Gillot, P.Y., Villari, L., 1980. K/AR geochronological data on the Aeolian Arc Volcanism. A preliminary report. IIV Open File Report, 3/80.
Gordeev, E.I., Senyukov, S.L., 2003. Seismic activity at Koryakski Volcano in 1994: hybrid seismic events and their implications for forecasting volcanic activity. J. Volcanol. Geotherm. Res. 128 (1–3), 225–232.
Got, J.L., Fréchet, J., Klein, F.W., 1994. Deep fault plane geometry inferred from multiplet relative relocation beneath the south flank of Kilauea. J. Geophys. Res. 99, 15375–15386.
Herring, T.A., King, R.W., McKlusky, S.C., 2006a. GAMIT Reference Manual: GPS Analysis at MIT, Version 10.3. Massachusetts Institute of Technology, Cambridge, MA.
Herring, T.A., King, R.W., McKlusky, S.C., 2006b. GLOBK reference manual: Global Kalman filter VLBI and GPS Analysis Program, Version 10.3, Massachusetts Institute of Technology, Cambridge, MA.
Hornig-Kjarsgaard, I., Keller, J., Koberski, U., Stadlbauer, E., Francalanci, L., Lenhart, R., 1993. Geology, stratigraphy and volcanological evolution of the island of Stromboli, Aeolian arc, Italy. Acta Vulcanol. 3, 21–68.
Irwan, M., Kimata, F., Fujii, N., 2006. Time dependent modeling of magma intrusion during the early stage of the 2000 Miyakejiama activity. J. Volcanol. Geotherm. Res. 150, 202–212.
Jeffreys, H., Bullen, K.E., 1967. Seismological Tables. British Association, Gray-Milne Trust.
Keller, J., Hornig-Kjarsgaard, I., Koberski, U., Stadlbauer, E., Lenhart, R., 1993. Geological map of the island of Stromboli. Acta Vulcanol. 3, 3.
La Rocca, M., Galluzzo, D., Saccorotti, G., Tinti, S., Cimini, G.B., Del Pezzo, E., 2004. Seismic signals associated with landslides and with a tsunami at Stromboli volcano, Italy. Bull. Seismol. Soc. Am. vol. 94 (5), 1850–1867 October 2004.
Lahr, J.C., 1989. HYPOELLIPSE/VERSION 2.0: A computer program for determining local earthquake hypocentral parameters, magnitude and first motion pattern. U.S. Geol. Surv., Open-File Rep., 89/116, 81 pp.
Lahr, J.C., Chouet, B.A., Stephens, C.D., Power, J.A., Page, R.A., 1994. Earthquake classification, location, and error analysis in a volcanic environment: implications for the magmatic system of the 1989–1990 eruptions at Redoubt volcano, Alaska. J. Volcanol. Geotherm. Res. 62, 137–151.
Landi, P., Francalanci, L., Pompilio, M., Rosi, M., Corsaro, R.A., Petrone, C.M., Nardini, I., Miraglia, L., 2006. The December 2002–July 2003 effusive event at Stromboli volcano, Italy: insights into the shallow plumbing system by petrochemical studies. J. Volcanol. Geotherm. Res. 155, 263–284.
Langer, H., Falsaperla, S., 2003. Seismic monitoring at Stromboli volcano (Italy): a case study for data reduction and parameter extraction. J. Volcanol. Geotherm. Res. 128, 233–245.
Livieratos, E., 1980. Crustal strains using geodetic methods. Quaterniones Geodaesiae 3, 191–211 2004GL021549.
Mattia, M., Rossi, M., Guglielmino, F., Aloisi, M., Bock, Y., 2004. The shallow plumbing system of Stromboli Island as imaged from 1 Hz instantaneous GPS positions. Geophys. Res. Lett. 31, L24610. doi:10.1029/2004GL021281.
Montalbetti, J.F., Kanasewich, E.R., 1970. Enhancement of teleseismic body waves with a polarization filter. Geophys. J. R. Astron. Soc. 21, 119–129.
Morelli, C., Giese, P., Cassinis, R., Colombi, B., Guerra, I., Luongo, G., Scarascia, S., Shutte, K.G., 1975. Crustal structure of Southern Italy. A seismic refraction profile between Puglia–Calabria–Sicily. Boll. Geofis. Teor. Appl. 18, 183–210.
Neri, G., Barberi, G., Orecchio, B., Aloisi, M., 2002. Seismotomography of the crust in the transition zone between the southern Tyrrhenian and Sicilian tectonic domains. Geophys. Res. Lett. 29 (23), 2135. doi:10.1029/2002GL015562.
Okada, Y., 1985. Surface deformation due to shear and tensile faults in half-space. Bull. Seismol. Soc. Am. 75, 1135–1154.
Pasquarè, G., Francalanci, L., Garduño, V.H., Tibaldi, A., 1993. Structure and geological evolution of the Stromboli volcano, Aeolian islands, Italy. Acta Vulcanol. 3, 79–89.
Patané, D., Ferrari, F., 1997. SEISMPOL: a visual basic computer program for interactive and automatic earthquake waveform analysis. Computer & Geoscience 23 (9), 1005–1012.
Poupinet, G., Ellsworth, W.L., Frechet, J., 1984. Monitoring velocity variations in the crust using earthquake doublets: an application to the Calaveras fault, California. J. Geophys. Res. 89, 5719–5731.
Scandone, P., 1979. Origin of the Tyrrhenian Sea and Calabrian Arc. Boll. Soc. Geol. It. 98, 27–34.
Spakman, W., 1990. Tomographic images of the upper mantle below central Europe and the Mediterranean. Terra Nova 2, 542–553.
Tarantola, A., Valette, B., 1982. Generalized nonlinear inverse problems solved using the least squares criterion. Rev. Geophys. Space 20 (2), 219–232.
Tibaldi, A., 2001. Multiple sector collapses at Stromboli volcano, Italy: how they work. Bull. Volcanol. 63, 112–125.
Tsujiura, M., 1983. Characteristic frequencies for earthquake families and their tectonic implications: evidences from earthquake swarms in the Kanto District, Japan. Pure Appl. Geophys. 121, 573–600.
Vaggelli, G., Francalanci, L., Ruggieri, G., Testi, S., 2003. Persistent polybaric rests of calcalkaline magmas at Stromboli volcano, Italy: pressure data from fluid inclusions in restitic quartzite nodules. Bull. Volcanol. (Heidelberg, Germania) 65, 385–404. doi:10.1007/s00445-002-0264-8.
Zanchi, A., Francalanci, L., 1989. Analisi geologico-strutturale dell'Isola di Stromboli: alcune considerazioni preliminari. Boll. G.N.V. 2, 1027–1044.